Specialized wavefront sensors for adaptive optics[1]

D.R. Neal
J.D. Mansell
J.K. Gruetzner
R. Morgan
M.E. Warren
Sandia National Laboratories, P.O. Box 5800, Albuquerque, NM 87185-1423

ABSTRACT

The performance of an adaptive optical system is strongly dependent upon correctly measuring the wavefront of the arriving light. The most common wavefront measurement techniques used to date are the shearing interferometer and the Shack-Hartmann sensor. Shack-Hartmann sensors rely on the use of lenslet arrays to sample the aperture appropriately. These have traditionally been constructed using MLM or step and repeat technology, and more recently with binary optics technology. Diffractive optics fabrication methodology can be used to remove some of the limitations of the previous technologies and can allow for low-cost production of sophisticated elements.

We have investigated several different specialized wavefront sensor configurations using both Shack-Hartmann and shearing interferometer principles. We have taken advantage of the arbitrary nature of these elements to match pupil shapes of detector and telescope aperture and to introduce magnification between the lenslet array and the detector. We have fabricated elements that facilitate matching the sampling to the current atmospheric conditions. The sensors were designed using a far-field diffraction model and a photolithography layout program. They were fabricated using photolithography and RIE etching. Several different designs will be presented with some experimental results from a small-scale adaptive optics brass-board.

Keywords: Wavefront sensor, Adaptive optics, Lenslet arrays, Binary optics, diffractive optics, pupil remapping

1. INTRODUCTION

Several different types of wavefront sensors have been used effectively for adaptive optics systems. These include Shack-Hartmann, curvature and shearing interferometer. Each of these sensors has advantages and may be customized for the particular system. For example, curvature sensors have been coupled to bimorph deformable mirrors to take advantage of sensing the same wavefront derivative that the mirror needs for control. Shearing systems have been applied to segmented adaptive optics for tip/tilt and phase comparison of adjacent segments. For Shack-Hartmann sensors, the customization takes the form of selecting the number and arrangement of subapertures to match the deformable mirror.

A Shack-Hartmann sensor has several basic components: a lenslet array, a detector and data acquisition and analysis. Until recently there were relatively few techniques available for fabricating the lenslet arrays. However, with the advent of binary optics technology, many of these barriers have been removed.

Binary optics technology is the application of semiconductor manufacturing methods to the fabrication of optics. A lens or lens array is laid out on a computer CAD program and transferred to a photo-mask using an e-beam (or other) writing process. A series of photo-masks are used, in conjunction with various etch steps, to build up the structures of interest. This fabrication technique can be used to make arrays of lenses with ~1 μm features in completely arbitrary patterns. Lenslet arrays are straightforward to make with these methods, and can be extremely high quality with no dead space between elements.

By taking advantage of the arbitrary nature of binary optics, these lenslet arrays can be customized for the particular adaptive optic system. Since the design of the array is determined by the software layout program, there is no fabrication penalty for designing complicated or esoteric patterns or surface shapes. For example, an asphere is no harder to design and fabricate than a sphere. Similarly, the designer is not limited to a particular aperture shape, size or pattern. The optic array can be designed to map from the

[1] This work was supported by the United States Department of Energy under contract number DE-AC04-94L85000.

telescope or deformable mirror pupil to that of the detector. In some cases, intermediate optics can be eliminated or simplified.

For an adaptive optics system there are several areas where this remapping can be applied. Optical system apertures are usually round, while detectors are usually square. By remapping from a round to a square pupil using a binary optics approach, the detector fill factor can be improved. In addition, the spacing of actuators on the deformable mirror may be different in x-and y directions. These can also be adjusted. Further, often the size of the telescope pupil image is not the same as that of the detector, and relay imaging optics must be used. This can also be accomplished in the design of a proper binary optic.

The body of this paper presents examples of various customized lenslet arrays for Shack-Hartmann sensing and outlines the methodologies used in the design approach. We present examples of image size, aperture shape, segment shape, spot position and subaperture function remapping.

2. BINARY OPTICS BASED WAVEFRONT SENSORS

2.1 Binary optics fabrication

Figure 1 presents the basic fabrication sequence for making a binary optic. The desired surface shape is broken up into a series of discrete phase levels, with the overall shape approximated by these levels. These optics are binary only in the sense that they are made from discrete levels. Typically 16 level systems are used to make precision optics. The phase levels are fabricated in a digital fashion using a number of photolithography and etch steps. The masks for the photolithography process are designed using a customized CAD Program and commercial mask layout software. We are currently working on integrating the lens design functions into a low cost CAD program to allow rapid prototyping.

The advantage of binary optics is that the optical fabrication is not limited to spheres and simple surfaces. The total etch depth is limited to a few micrometers,. the minimum feature size to about 1 μm, and the total optic size is limited by the amount of computer storage available in the mask production computer. However, for many wavefront sensor applications these limitations are not often exceeded. It is straightforward to design and fabricate two dimensional arrays of lenses. The feature size does not become a problem unless the f# gets very low. For the high f# lenslet arrays usually specified for wavefront sensing, this is rarely a difficulty. Furthermore, the lenslet size is usually fairly close to the size of the detector, and thus large optics are not required. It should be pointed out that none of these limits are not hard and fast. Large binary optics have been produced, as well as extremely fast optics. Feature sizes less than 1 μm can be obtained using direct write e-beam or x-ray lithography. It is just more difficult and hence more expensive.

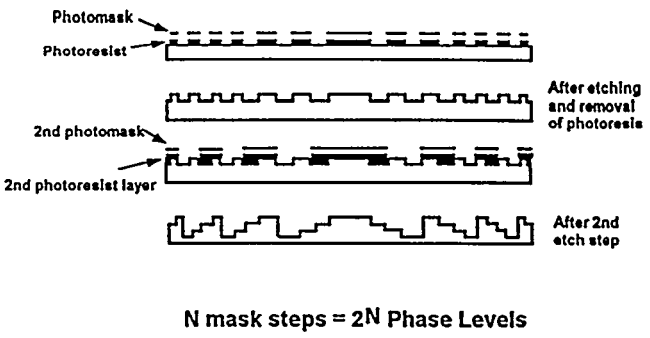

Figure 1 - Fabrication sequence for a four level binary optic.

The optical system can be laid out as an array of lenses (which is convenient for Hartmann sensing) or in other arbitrary arrangements. In fact, the arrangement of lenses does not have to be regular or continuous. We have used this to advantage for a number of other applications[1]. It is this arbitrary nature of the optical surface that will allow us to design customized wavefront sensors.

2.2 Wavefront sensor design

2.2.1 Lenslet arrays for Shack-Hartmann sensors

The Shack-Hartmann sensor is a primary application for binary optics, since it requires the fabrication of arrays of lenses. In fact, lenslet arrays were one of the first demonstrations of binary optics[2]. The total sag for a lenslet can be written:

$$s = \frac{d}{8f\#(n-1)} \qquad (1)$$

where d is the lenslet diameter, n is the index of refraction and s is the sag. For a typical $f\#$ 100 lens, with 32 lenslets per cm, this corresponds to a total sag of 0.85 μm. While this is more than a wave for light in the visible spectrum, it is straightforward to build a lens with the complete contour.

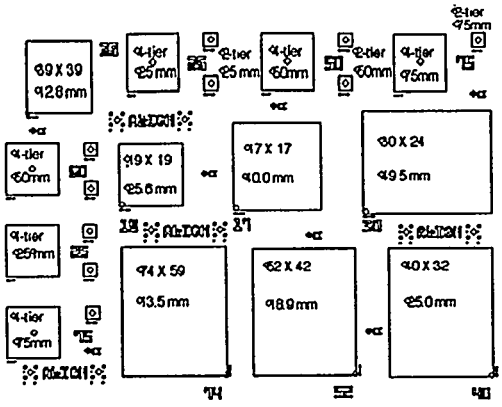

Figure 2 - Arrangement for binary optic with 23 different lenslet arrays on a single substrate.

With a 16 phase level fabrication sequence, the lens RMS roughness would be <0.02 μm. For visible light (0.5 mm) this is better than λ/20 and has an efficiency of > 99%. Even much larger or faster lenses would have adequate performance using this technique. Alternatively, a Fresnel lens could be laid out. This would have the advantage of maximum efficiency at a particular wavelength, but would be limited to an extremely narrow band because of strong chromatic aberration.

This lenslet array is also designed to have *zero* dead space between lenses. The lenslets are placed accurately to a (typically) 0.1 μm grid. Since the features are specified to 1 μm accuracy, there is no space in between lenses, and hence the array has a 100% fill factor. For wavefront sensing this can be important because any leakage light will degrade the noise performance of the total system.

Because of the 100% fill factor, and the high efficiency attainable for lenses that will operate over a broad range of wavelengths, binary optics is ideally suited for wavefront sensing applications.

The arrangement of lenslet arrays laid out on a typical 2 inch diameter substrate is presented in Fig. 2. There are 23 different optics on this substrate in total. For our research purposes, we laid out designs to test a number of concepts, in addition to the specific lenslet arrays for a variety of different cameras. This suggests one simple method for customizing the lenslet array to the adaptive optic. As the wavefront error that is measured varies, the best lenslet array for the measurement purpose is selected from among a variety of choices on the same substrate

For one of the cameras (Pulnix TM645) four different lenslet arrays were designed and fabricated on the same substrate. This gave us the capability of changing the

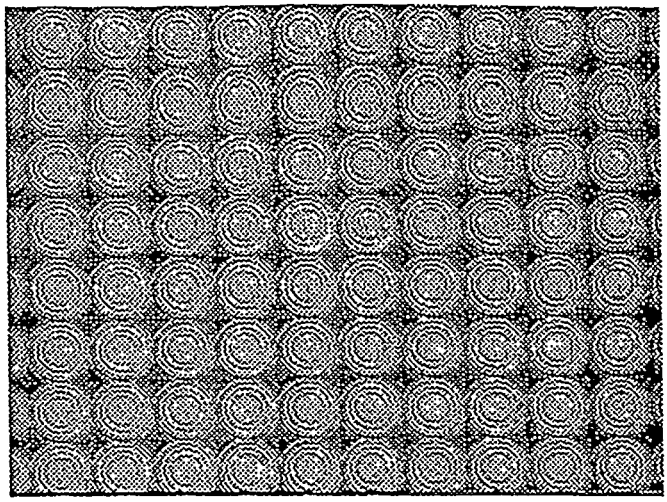

Figure 3 - Binary optic lenslet array fabricated with photolithography and reactive ion etching. The lenslets are 250 mm diameter with 25 mm focal length.

wavefront sensor resolution, sensitivity and dynamic range to match the conditions of the expected aberration. A simple mechanical alignment system was used to switch between lenslet arrays in a rapid fashion. In this way we were able to use the optimum sampling for a very wide variety of measurement applications including OPO laser beam quality measurement, automotive glass surface flatness variations and laboratory turbulence[3].

For astronomical applications, it would be possible to automate this process and select wavefront sensors that are appropriate for different atmospheric conditions. This might allow the optimal sampling/r_0 to be maintained even as the atmosphere varied. The lenslet arrays could be arranged to allow easy transition from one to the other using stepper motors or other automated mechanism. This may work best for wavefront sensors that use modal reconstructors, since it would not result in a direct mapping of lenslet aperture to deformable mirror actuator arrangement. For some adaptive optics systems this may be feasible.

3. NEURAL NETWORK REMAPPING SYSTEM

Since the overall goal of this work was to develop methodologies for remapping the pupil for specific applications, a general purpose re-mapping engine was needed. This engine would need to optimally remap from one space to the next while improving or maintaining an overall figure of merit. Since this task is primarily one of mapping from one geometric space to another, the engine was built to accept input an output from a commercial low cost CAD package[4]. This has significant advantages in the

ease and simplicity of the design, and since these CAD programs can be used directly to produce the photo-masks, the entire process is greatly simplified.

While a conventional least squares minimization routine could have been used for this purpose, the large number of potential mappings lends itself well to neural net solution techniques. We have adopted several recent neural net algorithms as the core of the remapping engine.

3.1 Introduction

The binary optics are fabricated using a reactive ion etch (RIE) process because of its anisotropic nature. Beyond an etch depth of 1.5 microns, the conventional photolithographic masks begin to deteriorate, so the maximum sagitus of an optic fabricated using an RIE machine is set at this depth. For some applications this is less of a limitation because the optic can be designed for a certain wavelength and a Fresnel structure can be implemented, but some applications require a wide range of wavelengths, so a Fresnel structure would lead to reduced performance. Using the paraxial-ray approximation and the thin lens approximation, the sagitus can be shown to be approximately,

$$s = \frac{r^2}{2f(n-1)} \qquad (2)$$

This then becomes the major figure of merit for the system design. In order to meet the low sagitus requirement, the off-axis radius must be minimized. For some geometries this is straightforward, but for more complex geometries, a general system had to be designed to solve this problem. Work by Takefuji[5] showed that parallel feedback neural networks were particularly good at this type of optimization. This network is based upon his work.

3.2 The Algorithm

The network is setup such that there is an array of inputs and an array of outputs. There is initially a random mapping from every input to one output. Every output neuron is "connected" to a number of its neighbors. In every iteration, each output neuron evaluates the error associated with switching mappings with each of its neighbors. If the error is less than the error associated with the current arrangement, the mapping changes. The error function used to evaluate the error associated with a mapping from input *i* to output j is given by,

$$ERR_{ij} = \left[x_i - x_j\right]^2 + \left[y_i - y_j\right]^2 \qquad (3)$$

which is simply the square of the Euclidean distance between the two points on the Cartesian coordinate plane. Other factors could be added to this error function to make it more flexible. For example, if it was desired to add a net force to the movement of the neurons toward the top of the output plane, a factor of (TOP_y-y_j) could be multiplied by the distance to weight the top as a lower error than the bottom.

The movement function of this network is given by,

$$\frac{\partial U}{\partial t} = \left[ERR_{kl} - ERR_{ij}\right] - \left[ERR_{kj} - ERR_{il}\right] \qquad (4)$$

which is simply the gradient of the error space. In other words, the movement function simply evaluates the change in error associated with switching the mapping between the (*i*->j) and the (k->l) cases. The mapping changes only if there is a reduction in error. The network keeps iterating until the movement of the neurons has stopped. At this time nothing has been done to address local minima because they have not been shown to be a problem in the experiments that have currently been performed, but it is foreseen that some steps (like "kicking" the converged configuration with some random switches) might be necessary.

3.2.1 Autoscaling

Since sagitus is such a limitation with these optics, anything that can be done to minimize the effective radius is necessary and warranted. Because often the input plane is a different size than the output plane, automatic scaling of the input plane to match the output plane was allowed. This procedure will necessitate scaling optics, but will preserve the power of the pupil remapping. Figure 4 is a depiction of the error associated with a converged network versus a scaling factor that was multiplied by the output plane.

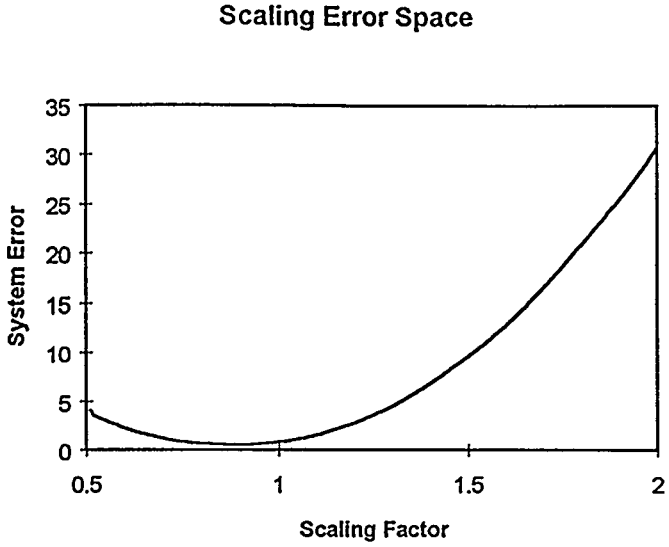

Figure 4 - The error space of a neural network with respect to scale factor.

In this case, a definite minimum can be seen around 0.9. The error space is quite smooth, but local minima were anticipated, so two different search techniques were implemented. First a brute force method simply asks the user for a starting point, stopping point, and the resolution of the scan. A second method was implemented based upon the GESA (guided evolutionary simulated annealing) algorithm[6] [2]. Starting at a scaling of 1.0, ten random attempts are made at a radius of 1.0 from the current best solution. Another ten attempts are made at a radius of 0.5 from the previous solution. Every ten iterations, the search radius halves. This continues for as many iterations as the user requests. At the end of the iterations, the best solution is reported. The advantage of a GESA search is that a finer resolution is attainable more quickly than with a series of brute force searches. Also GESA tends to be better at avoiding local minima than the brute force technique.

4. CUSTOMIZED LENSLET ARRAYS

In order to fabricate the lenslet arrays, masks must be generated from the mappings. A computer program was written to accomplish this task. The program used the sagitus equation to determine the height and then finds the radius associated with this sagitus. From the radius the program finds out where that radius intersects the line segments defining the shape of the lenslet. Finally, from these intercepts, a depiction of the lens can be made. This

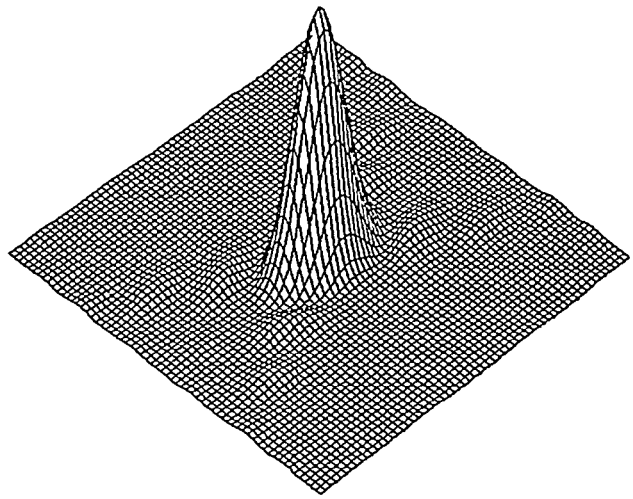

Figure 6 - Far field diffraction pattern from a single diamond shaped aperture.

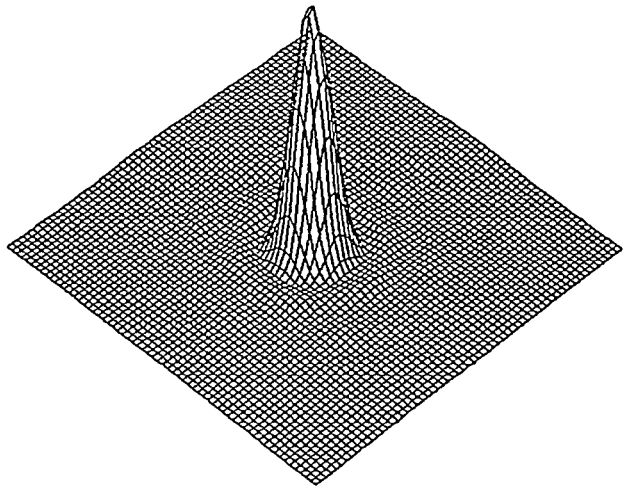

Figure 5 - Far field diffraction pattern from an array of hexagonal apertures.

section describes four types of custom lenslets that can be fabricated using this technique.

4.1 Lenslet Shape

One key element in designing a lenslet array for adaptive optics wavefront sensing is the arrangement of the actuators on the deformable mirror. For best performance on the wavefront reconstructor, this must be matched to the wavefront sensor. Typical actuator patterns are either rectangular, square or hexagonal, placing similar requirements on the lenslet array. While hexagonal or

square lenslet arrays are relatively straightforward, other shapes may provide best performance for a real system.

With binary optic pupil remapping, a custom lenslet array can readily be designed to match the exact pattern of actuators on the deformable mirror. While most of these patterns are regular, this is not a requirement. Figure 7

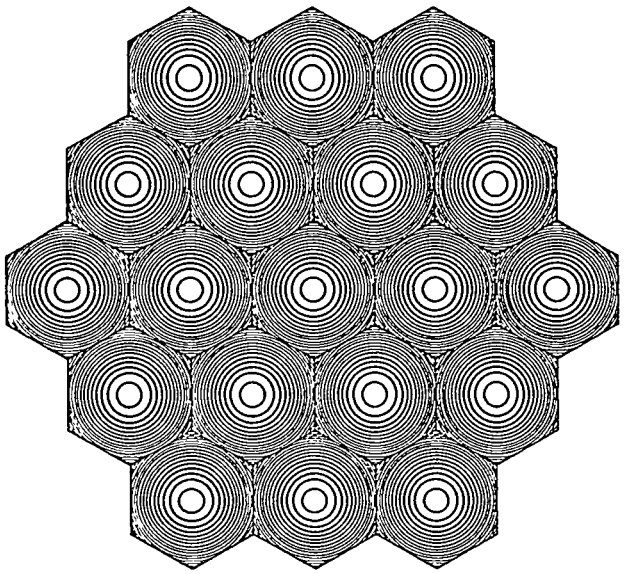

Figure 7 - Lenslet array using hexagonal shaped subapertures arranged telecentrically.

shows a diamond-shaped array of telecentric lenslets. The diamond shape is useful for deformable mirrors with hexagonal actuator spacing, where the actuators are at the nodes of the diamonds. Each wavefront sensor can be used to determine the net different x and y tilts directly, thereby simplifying the operations required by the wavefront reconstructor.

The size of the segments need not even be constant, and different size elements can be used to account for edge effects or for other know constraints imposed by the optical system or deformable mirror.

One key issue when changing the shape of the subaperture is the resulting diffraction pattern. While the diffraction patterns from common aperture shapes are well known and easily analyzed, this is not necessarily true for any arbitrary shape. The diffraction pattern of each element and the coherent addition of elements must be considered in the design. Figure 5 shows the modeled diffraction pattern of a hexagonal aperture[9]. Figure 6 presents the diffraction pattern from a single diamond shaped subaperture.

4.2 Focal Spot Spacing

For a hexagonal actuator deformable mirror the spacing of focal spots in the x- direction is different from the spacing in the y-direction by 15%, with every other row shifted by half the horizontal spacing. While it is easy to account for the row shift, the different spacing means that the focal spots cannot be lined up with the same pixels for each successive row. This can introduce some estimation error in the centroiding algorithms, and it requires that the centroiding boxes be adjusted periodically during processing. For a diamond shaped aperture, this problem

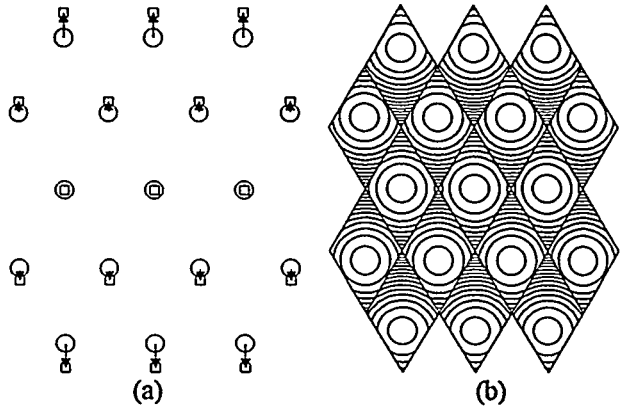

Figure 9 -Diamond shaped lenslet array with the focal spot positions remapped to a regular grid. (a) Lenslet to detector mapping arrangement. Circles represent the lenslet array aperture and squares are the detector plane arrangement. (b) Resulting lenslet array design showing lens contours.

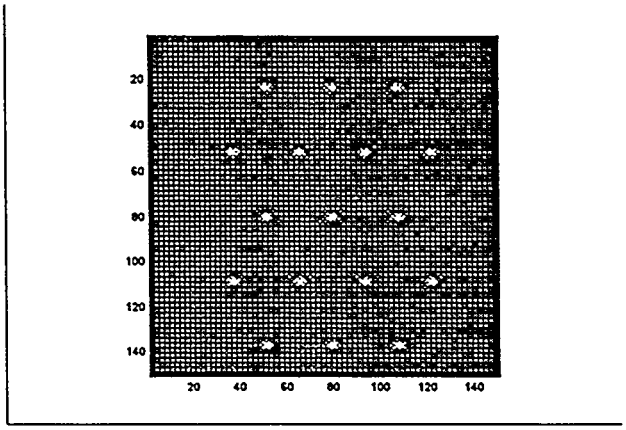

Figure 8 - Diffraction modeling of the optic design in Figure 7.

gets even worse. The difference in the x- and y-directions is 73%, and so large adjustments must be made.

To overcome this problem, each of the lenslets is allowed to be used off-axis. Thus the spot spacing can be placed on a regular grid with the same spacings in x and y, even though the lenslet array itself is not so regular. This is depicted in Figure 9. Figure 8 shows the modeled diffraction pattern of this optic.

Using a lenslet off-axis places an additional requirement on the binary optic. The sag for an off-axis element can be significantly greater than that for an on-axis one. Thus the sag is an important criteria in the design of a lenslet array. Ultimately, it is the sag that limits the performance, since only fairly small total etch depths are possible using the reactive-ion etching technique discussed in Section 2.1. This problem may be overcome for systems where laser light (or narrowband light) is usable by implementing a suitable Fresnel lens.

4.3 Image Re-sizing

One of the key requirements in an adaptive optical system is that the lenslet array be properly matched to the detector array. This involves choosing the appropriate f# so that the correct size spots can be generated on the detector. The system magnification and lenslet diameter can then be mapped back to the telescope system aperture to determine the overall sensitivity and dynamic range. Often this is done using an intermediate pupil image and relay imaging optics to select the appropriate parameters. This relay imaging system can introduce errors causes by improper alignment and inherent errors in the relay optics. While these errors can often be accounted for through calibration, this adds to the processing burden of the system. Using a system with off-axis elements as shown in Figure 10, the re-imaging can be performed by the lenslet array itself.

It is important to note that building the re-imaging into the binary optic is exactly equivalent to using an external lens arrangement. In both cases the dynamic range depends upon the overall system magnification, and the spacing of spots on the detector. Thus the maximum dynamic range can be written:

$$\theta_{max} = \frac{d}{2Mf} \qquad (5)$$

where M is the system magnification, f is the lenslet focal length and d is the spot spacing on the detector. For telecentric lenslet arrays the spot spacing and the detector width are the same, whereas for re-sized lenslet arrays, the two are different by the re-imaging magnification.

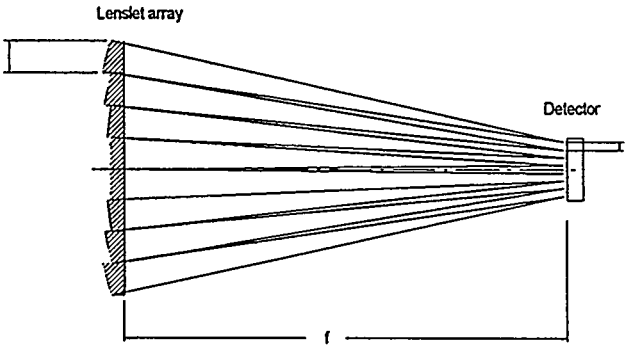

Figure 10 - Resizing can be built into the binary optic lenslet array. Parameters for a typical re-sized lenslet array are shown.

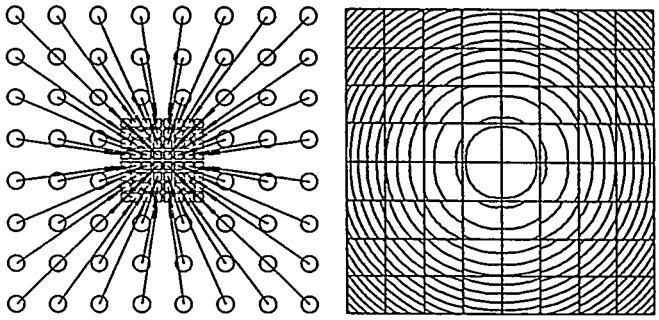

Figure 11 - Remapping from a 4 mm diameter 8x8 lenslet array down to a 1 mm square detector to eliminate the need for a reimaging lens between lenslet array and detector. (a) depicts the mapping function with circle denoting the pupil plane and squares the detector plane and (b) shows the resulting lens contour profile.

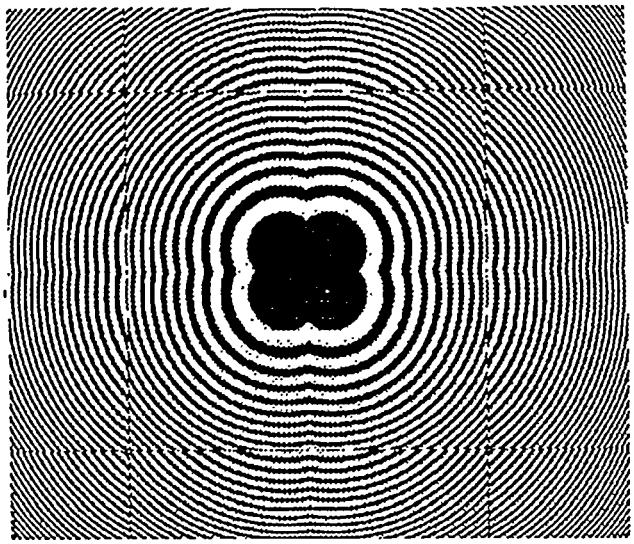

Figure 12 - (a) Center portion of the mask design for a 4:1 re-sized lenslet array. The large sag of this system necessitated the use of Fresnel lens structures.

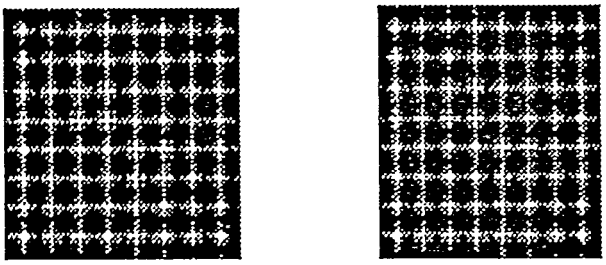

(a) (b)

Figure 14 - Far field simulations of re-sized lenslet array. (a) Fourier transform model and (b) linear superposition analytical model. The simulation uses the actual expected detector resolution.

Figure 12 and Figure 11 depict a system for an 8x8 lenslet array that was designed for a beam combining adaptive optical system[7]. For this system a low pixel count (64x64) 1 mm detector was required for high frame rate operation. Mechanical constraints led to a minimum focal length of 7.5 mm, which placed the lenslet f# at 58.6. This created focal plane spots that were 74 μm diameter, which corresponds to 4.6 pixels. Since each spot needed to be contained in an 8x8 box, this left little dynamic range, and would likely lead to coherent coupling with adjacent areas. Reimaging was clearly needed.

Three alternative designs were considered: a 4 mm, an 8 mm and a 50 mm diameter lenslet array. The 50 mm array had the advantage that no intermediate reimaging was necessary, since the deformable mirror itself was 50 mm

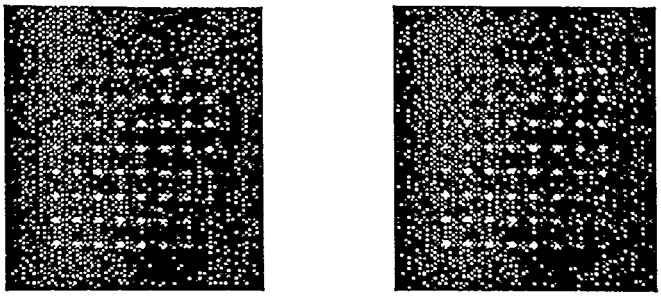

(a) (b)

Figure 13 -CCD camera image from 4:1 re-sized lenslet array. (a) A diagonal intensity band structure is present, even after AR coating (b).

diameter. However, the very large magnification (50:1) led to an extremely large off-axis sag and very small feature size. The large area of this device also would preclude making several optics at once and would stretch the amount of available memory in the mask making machines.

Both the 4 mm and 8 mm systems were laid out. The 8 mm system could not be fabricated because of memory limitations in the mask writer, so only the 4 mm system was made. This element was intended to be used at an intermediate image plane that was demagnified from the 50 mm deformable mirror size down to 4 mm. The optic performed the rest of the reimaging down to the 1 mm square detector with a 17 mm focal length.

This element was fabricated using the process described in Section 2.1. A portion of the mask design is shown in Figure 12. Figure 13 shows a typical far-field image from the fabricated element. The initial element was fabricated using a thin (2 mm thick) substrate with a ~30" wedge. Reflections from the back surface of this substrate caused a strong interference effect in the resultant image, resulting in a diagonal band structure in the intensity. This structure was eliminated by AR coating the back side of the optic or by using a thicker substrate. These images were found to have excellent agreement with diffractive models using both linear superposition of analytic solutions[8] and Fourier transform[9] far-field diffraction.

4.4 Aperture Shape

One key feature of most optical systems is that the optical system is round, while detectors are typically square. This leads, in general, to a mismatch between the optical system pupil shape and the detector. This usually leads to some portion of the detector being poorly utilized. For large obscuration cassegrain telescopes this can be particularly bad, with unused zones both in the corners and the middle of the field. Various customized detectors have been

developed to overcome these problems, however they are extremely custom and expensive.

Using pupil remapping, however, it is possible to map the circular aperture to the square detector. Figure 15 shows an optics designed to reduce a circle six squares in diameter to a 5x5 grid. Figure 17 shows the diffraction modeling of the optic. The program was allowed to autoscale using the GESA algorithm and found that the best proportion between the two was for the output to be 72% of the input size.

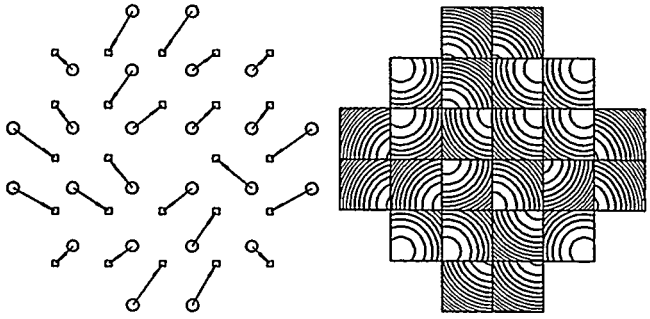

Figure 15 - Circular array mapped to a square grid.

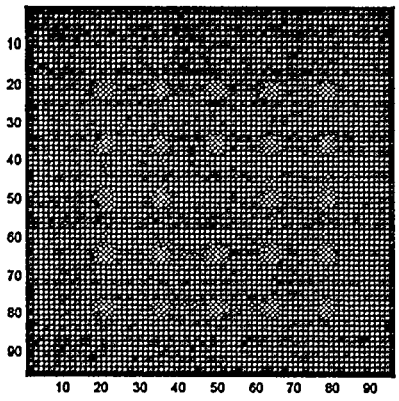

Figure 17 - Diffraction modeling of the circular array mapped to a square grid in Figure 15. A focal length of 350 was used and the size of the optic was approximately 4 by 4.

4.5 Hex DM remapped WFS

Using the above techniques, we have designed a series of wavefront sensor lenslet arrays for use on the 3.5m telescope at the Starfire Optical Range. The deformable mirror system is designed to be mounted on the telescope structure itself so that image rotation caused by the AZ/El mount will not be a problem. The deformable mirror is a ITEK hex actuator mirror with 97 actuators. The current system[10] uses an off-the-shelf hexagonal lenslet array from AOA. However, this array has too long a focal length for the known atmospheric conditions at SOR, and therefore must be replaced with an alternative.

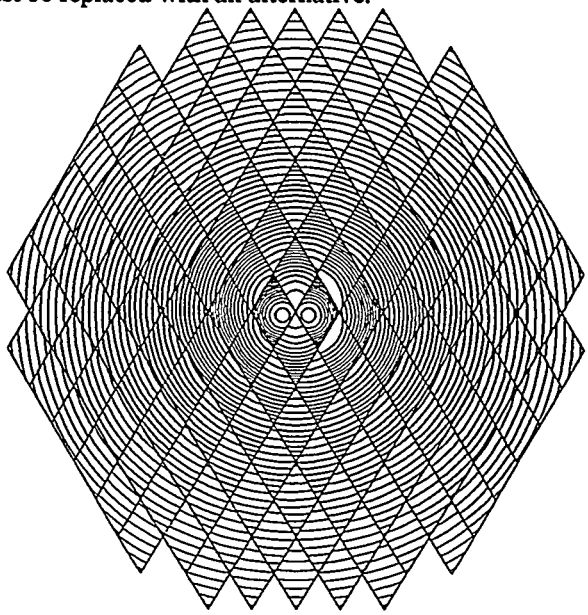

Figure 16 - The DM to detector pupil remapping that did not allow the algorithm to adjust the scale of the two apertures.

To that end we have considered all of the techniques presented in Sections 4.1 through 4.4 in various combinations. The segment shape was chosen as the diamond shape subaperture as shown in Figure 7 in order to optimize the wavefront reconstructor. An alternative hexagonal element has also been designed.

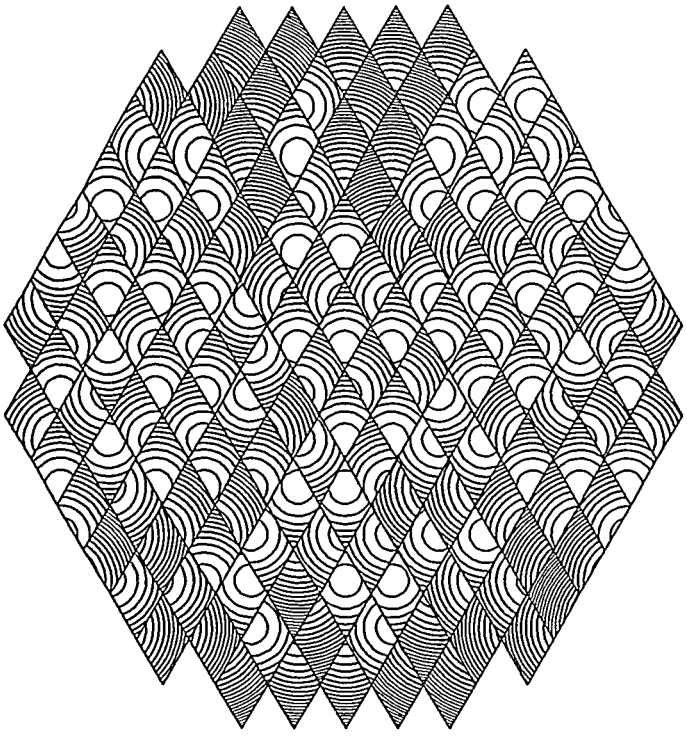

Figure 18 - Lenslet array design using optimal scaling. The image magnification is 0.9 from input to output.

As a first cut at the design, the neural net remapping algorithm was allowed to adjust all the parameters of the lenslet array, without regard for total sag. This yielded the mapping of Figure 16. The optical system reimages the DM down to a 5.5 mm pupil image for convenient diagnostics and the detector is a 64x64 1 mm CCD.
While this is an elegant solution to the overall problem, the total lens sag required is ~0.3 mm. The current binary optic fabrication techniques cannot achieve sags of this magnitude. For narrow band operation the optic could indeed be fabricated using Fresnel structures. In fact this may not prove to be too great a penalty, since a Fresnel structure has reasonable performance at up to 10% out of band. The primary affect is a reduction in the total Strehl ratio and overall spreading of the focal spot. For atmospheric imaging these affects might not be seriously limiting.

As an alternative to the design of Figure 16, we allowed the neural net engine to also adjust the scaling, based on the presumption that separate re-imaging optics would be used. This is not much of a penalty, since the current system already has reimaging optics designed and in place. The lenslet design and the neural network remapping are presented in Figure 18 and Figure 19 respectively.

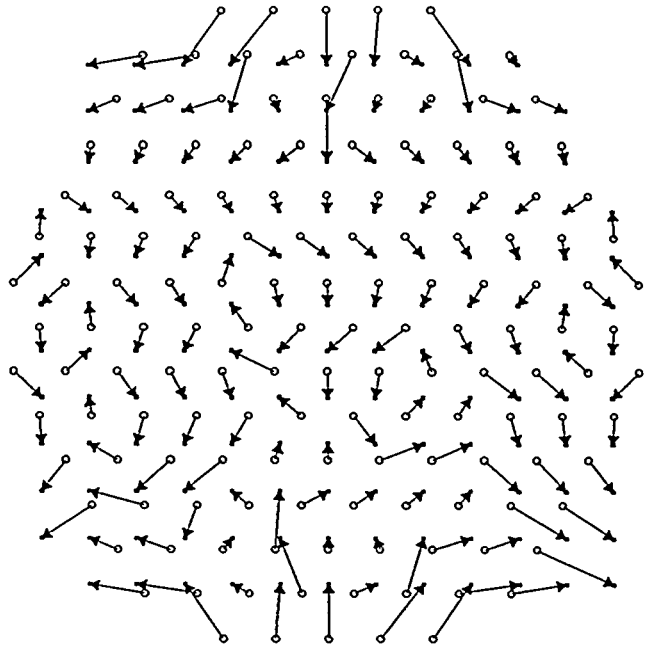

Figure 19 - Neural network remapping for the scaled case of the DM to the detector.

This element meets most of the design proposed design criteria. However, in order to achieve a low enough f#, the sag is still somewhat excessive.

5. CONCLUSIONS

Wavefront sensors like the Shack-Hartmann sensor depend on good lenslet arrays to couple the light into the detector. The technique of pupil remapping using binary optics is powerful because it allows the designer to use arbitrary lenslet shapes, to alter focal spot spacing, to resize the image, and to change the shape of the overall aperture. Binary optics has proven to be a good technique for fabricating lenslet arrays because it allows for a 100% fill factor, but they are limited by the current fabrication technology. Such limitations can be designed around using advanced computer techniques like neural networks and GESA.

---

[1] D. Neal *et al.* "A multi-tiered wavefront sensor," SPIE 2201 (1994).
[2] Veldkamp, Wilfrid B. "Binary Optics". Scientific American. V. 266, May 1992, p.92-7.
[3] D. Neal, R. Pierson, E. Chen, K. Bishop, L. McMackin, "One dimensional wavefront sensor development for tomographic flow measurements," SPIE 2546-48 (July 1995).
[4] EASYCAD for WINDOWS, Evolution computing, 1995.

[5] Takefuji, Yoshiyasu. Neural Network Parallel Computing. Kluwer Academic Publishers, Boston: 1992.
[6] Yip, Percy P. C. "Combinatorial optimization with use of guided evolutionary simulated annealing". IEEE Transactions on Neural Networks., Vol. 6, pp. 290-295 (March 1995).
[7] D. Neal , S. Tucker, *et al.*, "Multi-segment beam combining". SPIE 2534.
[8] D. Neal *et al.* "Optical and Control Modeling for Adaptative Beam-Combining Experiments". SPIE 2534.
[9] GLAD. Applied Optics Research. 1994.
[10] David Dayton. "Preliminary Optics Design 3.5 Meter Deformable Mirror Experiment". April 1995, Applied Technology Associates Informal Technical Report.

DISCLAIMER